An Instrumentation System Applied to Formation Flight

Walton R. Williamson, Mamoun F. Abdel-Hafez, Ihnseok Rhee, Eun-Jung Song, Jonathan D. Wolfe, *Member, IEEE*, David F. Chichka, *Member, IEEE*, and Jason L. Speyer, *Fellow, IEEE*

***Abstract*—As part of a NASA dryden autonomous formation flight program for improved drag reduction of multiple F/A-18 aircraft, a new instrument, the formation flight instrumentation system (FFIS), for the precise estimation of the relative position, velocity, and attitude between two moving aircraft without the aid of ground-based instruments, was developed. The FFIS uses a global position system (GPS) receiver and an inertial navigation sensor (INS) instrumentation package on each aircraft combined with a wireless communication system for sharing measurements between vehicles. An extended Kalman filter structure blends the outputs of each GPS/INS in a distributed manner so as to maximize the accuracy of the relative state estimates. Differential carrier phase GPS measurements are used to provide high accuracy relative range measurements to the filtering algorithm. A multiple hypothesis Wald test for estimating the integer ambiguity between the two moving vehicles was developed as part of this project. The FFIS was tested in a hardware-in-the-loop simulation (HIL Sim) before being tested in actual F-18 flight tests. Test results validated the FFIS performance. Flight test results showed that the Wald test accurately estimates the integer ambiguity and that relative range estimates using least squares provide accurate position estimates with a mean of approximately 7 cm and a standard deviation of 13 cm.**

***Index Terms*—Formation flight, global positioning system (GPS), inertial navigation sensor, instrumentation system, Kalman filtering.**

I. Introduction

A RECENT experiment at NASA Dryden Flight Research Center to develop autonomous formation flight for multiple aircraft required the development of an autonomous control system for performing complex, and extremely precise, maneuvers in formation. Flying in formation promises significant reduction in the cost of operation and increasing the range of aircraft in formation. Drag reduction is achieved through the alignment of aircraft vortices, as described in Hummel [1], and Chichka [2]. Flight tests during 2001 with two NASA F-18 aircrafts demonstrated a 20% drag reduction on the trailing aircraft [3]. An autonomous control system designed to maintain formation would improve long term duration and relieve pilot workload as well as enable formation flight for unpiloted air vehicles (UAVs).

In order to fly in formation and maximize drag reduction, the autonomous control system needs precise navigation and relative navigation between all aircraft in the formation. The proposed control algorithm for autonomous formation drag reduction seeks the point of maximum drag reduction online. This peak seeking control algorithm employs a gradient search [4], [5]. The gradient calculation requires precise transverse position estimation. The better the measurement of the transverse position, the more precisely the control algorithm will be able to maintain the maximum drag reduction. An instrumentation system was required to measure relative position of the aircraft in real-time in order to find and stay in the position of maximum drag reduction. One goal of the autonomous formation flight (AFF) experiment was to develop an instrumentation package that could reliably estimate the position, velocity, and attitude of each vehicle as well as the relative position, velocity, and attitude between two vehicles to high accuracy and distribute this information throughout the formation. The instrumentation could not use any ground-based measurements so that the formation control system only relied on equipment in the aircraft. A goal of centimeter-level accuracy was placed on the experiment since the size of the vortex was unknown at the start of the experiment.

Previous experiments in formation flight or precision relative navigation used carrier phase global position system (GPS) measurements compared to a fixed-base station such as car experiments, see Farrell [6]. Other solutions may combine fixed base stations with pseudolites such as the work in How [7]. Pseudolites were rejected since these instruments are redundant when compared with carrier phase GPS measurements and would require a large relative position change of one aircraft relative to the other in order to converge.

A more recent experiment involving landing F-18 aircraft on a carrier for the joint precision approach and landing system (JPALS) used a GPS/inertial navigation system (INS) on the carrier and a GPS/INS on the aircraft to measure relative distances and guide the aircraft to the carrier [8]. This program, similar in nature to the AFF program, developed requirements and a solution independently and in parallel with the results presented in this paper, although similar accuracy was achieved. The relative navigation system presented here differs in both hardware design and estimation algorithm design from the JPALS instrumentation. While both systems used an L1/L2 capable GPS receiver mixed with an inertial measurement unit (IMU), the hardware architecture differed in three substantial ways. The JPALS

Manuscript received September 21, 2004; revised November 7, 2005. Manuscript received in final form July 18, 2006. Recommended by Associate Editor D. A. Schoenwald. This work was supported by the NASA Dryden Flight Research Center under Contract NAS4–00051.

W. R. Williamson is with SySense, Inc., Pomona, CA 91768 USA (e-mail: walton@sysense.com).

M. F. Abdel-Hafez is with the American University of Sharjah, Sharjah, 26666, UAE (e-mail: mabdelhafez@aus.edu).

I. Rhee is with the Korea University of Technology and Education, Chunan Choongnam, 330-708, Korea.

E.-J. Song is with the Korea Aerospace Research Institute, Daejeon, 305-333, Korea (e-mail: ejsong@kari.re.kr).

J. Wolfe and J. L. Speyer is with the University of California, Los Angeles, CA 90095 USA (e-mail: wolfe@talus.seas.ucla.edu; speyer@seas.ucla.edu).

D. F. Chichka is with the George Washington University Academic Center, Washington, DC 20052 USA (e-mail: chichka@gwu.edu).

Digital Object Identifier 10.1109/TCST.2006.883241

NAPIE was based upon a shared memory architecture where it utilized a military communication system and measured the latency between the GPS measurements and IMU measurements but did not synchronize the two instruments. The carrier phase integer ambiguity problem between the aircraft and the carrier was solved using the Lambda Method [9], [10]. The relative position was then estimated using a least squares algorithm. The estimated relative position was blended with the IMU measurements in a loosely coupled manner.

In contrast, the formation flight instrumentation system (FFIS) designed for use in the experiment presented here, was built at UCLA with commercial off-the-shelf components. The FFIS used commercial quality GPS and IMU instruments on each aircraft. Measurements and estimates were shared between aircraft using an 802.11-b wireless network. The instrumentation system was designed as a distributed internal computer architecture which allowed a separation of task by processor. Each processor was assigned one of the communication tasks with the GPS, the IMU, the wireless system, and the F-18 control system being developed at Boeing Long Beach. However, the system, including the IMU sample rate, was synchronized to the GPS 1 pulse per second (PPS). This ensured that all FFIS units in the formation were also synchronized. The hardware implementation is described in more detail in Section III.

An extended Kalman filter (EKF) algorithm was developed to blend the GPS and INS instruments to provide the best estimate of relative position, velocity, and attitude. The algorithm distributes the computation load between the two aircrafts using a decentralized EKF structure. The INS is used to generate a reference trajectory for each aircraft. The GPS measurements are blended with the INS to correct for INS errors and IMU bias errors. Details of this algorithm are presented in Section IV.

High accuracy relative position estimation is achieved through the use of GPS carrier phase measurements to correct the INS. In order to process carrier phase measurements, the FFIS must first resolve the integer ambiguity between the two vehicles. UCLA developed a new method for resolving the integer ambiguity which does not require any ground-based instrumentation. This method, referred to as the Wald test, is briefly discussed in Section V.

As part of this development, the FFIS units were tested in a hardware-in-the-loop simulation (HIL Sim). The HIL Sim was an invaluable tool for developing software, assessing algorithm performance, and troubleshooting hardware before and during flight tests. The HIL Sim is described briefly in Section VI.

The FFIS was tested in flight on two F-18 aircraft during the fall of 2001. Over 15 flights took place as part of the research and development of the FFIS unit. FFIS real-time state estimates were telemetered to the ground and stored on board the FFIS during flight. The flight test results are presented in Section VII.

II. Nomenclature

$\bar{a}$	*A priori* estimate of a.
$\hat{a}$	*A posteriori* estimate of a.
δa	Estimation error of element a.
b_a	Vector of accelerometer biases.
b_g	Vector of gyro biases.

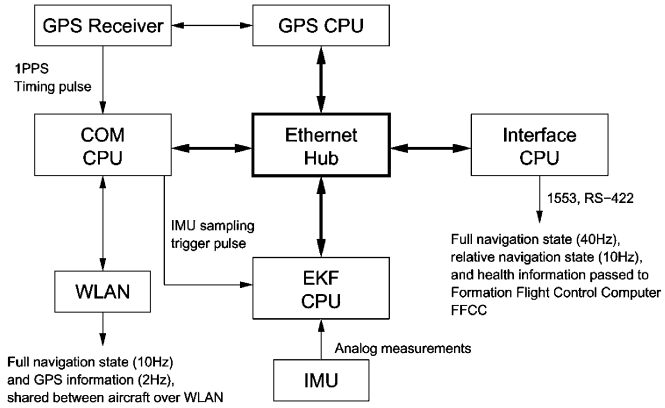

Fig. 1. FFIS hardware block diagram.

c	Speed of light in vacuum.
C_A^B	Cosine rotation matrix from the A frame to the B frame.
$E[a]$	Expected value of a.
f^B	Specific force vector in vehicle body coordinate frame.
L	Lever arm vector from the IMU to the GPS antenna in the body frame coordinates.
N	Unknown integer ambiguity vector.
P^E	Position vector in the earth-centered earth-fixed coordinate frame.
Q_A^B	Quaternion rotation from the A frame to the B frame.
t	Time.
V^E	Position vector in the Earth Centered Earth Fixed Coordinate Frame.
$\Delta(a)$	$(a)_{\mathrm{basevehicle}} - (a)_{\mathrm{rovervehicle}}$
λ	Carrier phase wavelength.
$\nabla\Delta(a)$	$\Delta(a)_{\mathrm{primesatellite}} - \Delta(a)_{\mathrm{secondarysatellites}}$.
$\tilde{\phi}$	GPS carrier phase measurements.
$\tilde{\rho}$	GPS code and Doppler measurements.
τ	GPS receiver clock bias.
ω_{AB}^C	Angular velocity vector of frame B relative to frame A represented in C frame.
$[()\times]$	Skew-symmetric vector cross product matrix.
$[\dot{a}]$	Time derivative of a.

III. FFIS Architecture

The FFIS consists of a GPS/INS instrumentation suite combined with a distributed computer architecture and a wireless communication system. Fig. 1 shows a block diagram of the system. For the formation flight experiment, one FFIS is placed on each aircraft. The FFIS supplies the formation control system with position, velocity, and attitude of the aircraft as well as the relative position, velocity, and attitude of the other aircraft.

The FFIS uses two types of instruments, a GPS, and an IMU. The GPS receiver is an Ashtech Z-12 Eurocard which provides both L1 and L2 carrier, code, and doppler measurements. The IMU is a Systron-Donner Motion Pak. This instrument provides

TABLE I
SYSTRON-DONNER MOTION PAK SPECIFICATIONS

	Accel	Gyro
Range	± 5 (g's)	± 50 ($^{\circ}/sec$)
Bandwidth	900 Hz	80 Hz
Noise (RMS)	0.0009 (g's)	0.036 ($^{\circ}/sec$)

three-axis linear acceleration and three-axis angular rate measurements in an analog output. Table I lists the noise level of the IMU according to manufacturers specifications.

The GPS antenna and the IMU are separated by over 3 m on the actual F-18. The GPS antenna is placed along the center line a few feet in front of the cockpit canopy. The IMU is located off of the center line and below the pilot in one of the F-18 instrumentation bays. The GPS antenna is located 3.56 m in front, 0.19 m starboard, and 0.81 m above the IMU. The instrument locations were measured precisely before the experiment.

In order to compute the state estimates in real-time while operating several asynchronous tasks, the FFIS was developed as a distributed system of CPUs communicating through ethernet. As shown in Fig. 1, the FFIS computer system uses four CPUs, on PC-104 format. The FFIS uses a stripped-down GNU/Linux operating system based on the 2.2.13 kernel on each CPU. The operating system and run-time software are stored on a solid state disk drive (disk-on-chip) device. The run-time software is developed in C using the GNU C compiler standard with Linux distributions.

The FFIS design, prototype, and software development were accomplished at UCLA. Boeing used the prototype in developing a system with the necessary robustness for the flight environment. The Boeing system used a distributed power system and internal cooling as well as a modified structure in order to allow the COTS parts to survive the full range of the flight environment. The FFIS hardware performed well during flight tests.

IV. FFIS ALGORITHM STRUCTURE

During operation, the navigation algorithms are based around the base/rover concept. In this scheme, one FFIS unit is designated as the base vehicle and the other is a rover vehicle. Both operate a standard strap-down INS. Normally, for a single vehicle, the GPS measurements are blended with the INS in order to correct the local state estimate for IMU bias drift [11]. Since GPS measurements contain errors common to both receivers, differential GPS techniques are adopted within a decentralized relative navigation scheme in order to eliminate the common errors in the GPS measurements and, therefore, improve the accuracy of the relative state estimates between the two vehicles.

As part of this scheme, each vehicle estimates the local state relative to Earth using the IMU measurements. The IMU measurements are integrated using a standard strap-down inertial navigation algorithm to form what is referred to as the INS [12]. This state is calculated at the IMU sample rate of 40 Hz. The solution is open-loop in the sense that the outputs of the IMU are integrated to form position and velocity estimates which are susceptible to errors induced from IMU biases.

For a single vehicle, the GPS measurements are used to correct the INS state for IMU errors in a seventeen state EKF. Both code and doppler measurements are processed to provide corrections to the INS. The states of the EKF are position, velocity, IMU accelerometer bias, gyro bias, GPS clock bias, GPS clock drift, and attitude. In the case of attitude, a reduced order quaternion model is used [12]. Performance results of this filter in ground tests are described in [12]–[14]. Flight test results are described in Section VII.

A. Strap-down Navigation

Each FFIS integrates the IMU measurements using the standard strap-down equations of motion. The INS state on each vehicle only depends upon the local IMU measurements. Details of the implementation are given in [12].

In implementation, the IMU measurements are first corrected for bias errors and then used to update the INS state. The INS state is calculated assuming constant IMU measurements over the interval (25 ms) and integrated using a standard fourth-order Runge–Kutta algorithm [15]. Note that both the base and rover use this scheme for calculating local state estimates. An EKF is used to correct the INS state for errors and to estimate biases in the IMU measurements. The two types of EKFs used are described in Section IV-B.

B. EKF for GPS/INS

This section defines the dynamics and measurement equation models for an EKF which estimates the correction to the INS state and the bias errors used in the previous section. The filter uses kinematic relationships to describe the dynamics of a single vehicle. Both pseudo range and doppler measurements are used to correct the state. This filter forms the basis of the relative navigation filter used in Section IV-C.

Since the filter was designed for use in a relative navigation scheme, and since the GPS measurements provide a common reference frame in the earth-centered earth-fixed (ECEF) coordinate frame, the EKF defined here calculates the error in the navigation state rotated to the ECEF coordinate frame. The continuous time dynamics are defined as follows:

$$\begin{aligned} \dot{P}^E &= V^E \\ \dot{V}^E &= C_B^E f^B - 2\omega_{iE}^E \times V^E + G^E \\ \dot{Q}_B^E &= \frac{1}{2}\Omega_{EB}^B Q_B^E \end{aligned} \tag{1}$$

where G^E is the gravity vector in the ECEF coordinate frame. The Ω_{EB}^B term is the quaternion angular velocity term defined in (2) and using the total angular velocity of the vehicle relative to the ECEF coordinate frame measured in the body axis frame of the vehicle $\left(\omega_{EB}^B\right)$

$$\Omega = \begin{bmatrix} 0 & -\omega_x & -\omega_y & -\omega_z \\ \omega_x & 0 & \omega_z & -\omega_y \\ \omega_y & -\omega_z & 0 & \omega_x \\ \omega_z & \omega_y & -\omega_x & 0 \end{bmatrix}, \qquad \vec{\omega} = \begin{bmatrix} \omega_x \\ \omega_y \\ \omega_z \end{bmatrix}. \tag{2}$$

In addition, it is desired to estimate the bias in the accelerometers and angular rate gyros. Since the filter will be designed using a tightly coupled GPS methodology, the GPS clock bias and clock drift are also estimated. These terms will be modeled as a Brownian Motion process.

The state for the EKF is comprised of the position, and velocity in the ECEF frame, the attitude between the body frame and the ECEF frame, and the measurement bias errors in the accelerometers, gyros, and GPS receiver clock. Assuming an *a priori* estimated state, the error in each of these states relative to the true values may be defined as follows:

$$\begin{aligned}\bar{P}^E &= P^E + \delta P\\ \bar{V}^E &= V^E + \delta V\\ \bar{b}_a &= b_a + \delta b_a\\ \bar{b}_g &= b_g + \delta b_g\\ C_B^{\bar{E}} &= C_E^{\bar{E}} C_B^E\\ c\bar{\tau} &= c\tau + c\delta\tau\\ c\bar{\dot{\tau}} &= c\dot{\tau} + c\delta\dot{\tau}.\end{aligned} \tag{3}$$

The $C_E^{\bar{E}}$ represents the error in the rotation matrix. To first order, the rotation matrix $C_E^{\bar{E}}$ is assumed to consist of small angles and may be defined as follows [16]:

$$C_E^{\bar{E}} = \left(I - 2\left[\delta q_B^E \times\right]\right) \tag{4}$$

where δq_B^E is the error in the estimated quaternion defined as: $\delta q_B^E = \begin{bmatrix}\delta q_1 & \delta q_2 & \delta q_3\end{bmatrix}^T$. The last quaternion term is neglected to first order, but is recalculated using the quaternion constraint equation: $1 = \sqrt{q_1^2 + q_2^2 + q_3^3 + q_4^4}$.

The IMU measurements are modelled as follows:

$$\bar{f}^B = f^B + b_a + w_a, \qquad \bar{\omega}_{iB}^B = \omega_{iB}^B + b_g + w_g \tag{5}$$

where w_a and w_g are assumed zero mean, Gaussian distributed random variables with covariances W_a and W_g, and b_a and b_g are biases modelled as Brownian Motion processes to ensure that the filter remains open.

Using these definitions, the EKF is constructed to estimate the *error* in the estimated state. This error state is defined as follows:

$$\delta x = \begin{bmatrix}\delta P^E & \delta V^E & \delta q_B^E & \delta b_a & \delta b_g & \delta\tau & \delta\dot{\tau}\end{bmatrix}^T. \tag{6}$$

The basic dynamic equation is represented simply as $\delta\dot{x} = A\delta x + w$. The δx term represents the perturbation error in the navigation state. The A matrix is the linearized dynamics defined in [12] and [16]. The derivation is not repeated here for brevity, but may be analyzed by inserting the error relationships defined in (5), (4), and (3) into (1). The A matrix is given in (7). The process noise, w is a zero mean Gaussian with power spectral density W

$$A = \begin{bmatrix} 0 & I & 0 & 0 & 0 & 0 & 0\\ \nabla\bar{G}^e & -2\left[\omega_{iE}^E\right]^\times & -2\left[C_B^{\bar{E}}\bar{f}^B\right]^x & C_B^{\bar{E}} & 0 & 0 & 0\\ 0 & 0 & -\left[\omega_{iE}^E\right]^\times & 0 & \frac{1}{2}C_B^{\bar{E}} & 0 & 0\\ 0 & 0 & 0 & 0 & 0 & 0 & 0\\ 0 & 0 & 0 & 0 & 0 & 0 & 0\\ 0 & 0 & 0 & 0 & 0 & 0 & 1\\ 0 & 0 & 0 & 0 & 0 & 0 & 0\end{bmatrix}. \tag{7}$$

The measurement matrix is derived using standard GPS measurement equations such as those in [17] and [18]. Both code range and doppler are used in processing the EKF. The measurement equation is defined as $\tilde{\rho} = \bar{\rho} + H\delta x + v$. In this equation, $\tilde{\rho}$ includes both the code and doppler measurements, $\bar{\rho}$ is the *a priori* estimate of the range and range rate calculated from the navigation state, H is the measurement matrix for both the code and doppler measurements composed of partial derivatives of the pseudo measurements with respect to the position and velocity evaluated at the current state estimate. Details of the derivation may be found in [12] and [16]. The term v represents the measurement uncertainty for each type of measurement and is modelled as a zero-mean Gaussian with power spectral density V. Note that the size of H depends upon the number of GPS satellites in view. If n satellites are in view, then H is a $(2n) \times 17$ matrix. The GPS measurement matrix for satellite i is given in (8), where $H_p = ((P^E - P^i)/(\|P^E - P^i\|))$, $H_p = ((V^E - V^i)/(\|P^E - P^i\|))(I - H_p^T H_p)$, P^i is the position of the satellite, and V^i is the velocity of the satellite

$$H^i = \begin{bmatrix} H_p & 0 & 0 & 0 & 0 & 1 & 0\\ H_v & H_p & 0 & 0 & 0 & 1 & 0\end{bmatrix}. \tag{8}$$

These two models define the linear relationship used to form an EKF. The EKF equations in discrete time used are as follows [19]:

$$\delta\hat{x}_k = \delta\bar{x}_k + K_k(\tilde{\rho}_k - \bar{\rho}_k - H_k\delta\bar{x}_k) \tag{9}$$

$$K_k = M_k H_k^T (H_k M_k H_k^T + V_k)^{-1} \tag{10}$$

$$P_k = (I - K_k H_k) M_k \tag{11}$$

$$\Phi_{k+1,k} = \exp(A_k\Delta t) \approx I + A_k\Delta t \tag{12}$$

$$M_{k+1} = \Phi_k P_k \Phi_k^T + W_k \tag{13}$$

$$\delta\bar{x}_{k+1} = \Phi_{k+1,k}\delta\hat{x}_k. \tag{14}$$

In this discrete time system, the k variable denotes time. The terms V_k and W_k are variances associated with v and w, respectively. This system defines the basic model for estimation of the base vehicle system. Using this model as a basis, a more complex system may be defined which is used for relative navigation. This is described in Section IV-C.

C. Decentralized Model for Relative Navigation

For the relative navigation problem, both vehicle states are considered in order to find the optimal filter structure to minimize the error in both the absolute and relative state estimates. The state space model can be represented as the following:

$$\begin{bmatrix}\delta\dot{x}_1\\ \delta\dot{x}_2\end{bmatrix} = \begin{bmatrix}A_1 & 0\\ 0 & A_2\end{bmatrix}\begin{bmatrix}\delta x_1\\ \delta x_2\end{bmatrix} + \begin{bmatrix}\omega_1\\ \omega_2\end{bmatrix} \tag{15}$$

where x_1 and x_2 denote the error in the state of the base and rover vehicles, respectively. A_1 and A_2 are the state transition matrices corresponding to the linearized dynamics, and ω_1 and ω_2 are the process noise of the base and rover vehicles. Note that the dynamics are calculated based upon the trajectory of the local vehicle and are completely independent of each other.

No aerodynamic coupling between aircraft is modeled. The dynamics are based solely on kinematic relationships for this experiment. The process noise for the dynamics is modeled as

$$\omega_1 \sim (0, W_1), \qquad \omega 2 \sim N(0, W_2), \qquad E\left[\omega_1 \omega_2^T\right] = 0. \tag{16}$$

The total state size is now 34 as this state equation combines the error in both the base and rover vehicles. Note that the kinematics are completely independent of each other, which is the case for two independent vehicles.

The measurement model for the GPS code and doppler measurements may be represented as follows:

$$\begin{bmatrix} \tilde{\rho}_1 \\ \tilde{\rho}_2 \end{bmatrix} = \begin{bmatrix} H_1 & 0 \\ 0 & H_2 \end{bmatrix} \begin{bmatrix} \delta x_1 \\ \delta x_2 \end{bmatrix} + \begin{bmatrix} v_1 + b_c \\ v_2 + b_c \end{bmatrix} \tag{17}$$

where $\tilde{\rho}_1$ and $\tilde{\rho}_2$ represent the GPS code and doppler available to each vehicle, and the measurement noise v_1 and v_2 are modelled as independent, zero mean white Gaussian processes. The *a priori* estimates of range are not included in this formulation for convenience and ease of notation. The GPS common mode errors are included in the term b_c which enter into both measurements $\tilde{\rho}_1$ and $\tilde{\rho}_2$ and results in a large correlation between the two independent systems. The common mode errors are also known to be much larger than either of the local GPS receiver errors, v_1 or v_2.

While the EKF will compensate for this correlation, the noise still colors both vehicle states.

The goal of the experiment is to minimize the error in the relative state estimate defined as $\Delta x = x_1 - x_2$. If the difference in the relative error is minimized, then the relative state estimates will have better performance. A rotation of the the current state may be made so that the common mode measurement noise is removed. The rotation changes the states from x_1 and x_2 to x_1 and $\Delta \delta x$.

A similar rotation can be applied to the measurement states $\tilde{\rho}_1$ and $\tilde{\rho}_2$ to form the measurement states $\tilde{\rho}_1$ and $\Delta\tilde{\rho}$. In essence, the EKF uses the GPS measurements from one vehicle and the differential GPS measurements between the two vehicles as inputs. The result is more accurate relative state estimates in position, velocity, and attitude due to the elimination of the common mode GPS errors.

Applying this rotation systematically to the state space and measurement models of (15) and (17), we obtain

$$\begin{bmatrix} \delta \dot{x_1} \\ \Delta \delta \dot{x} \end{bmatrix} = \begin{bmatrix} A_1 & 0 \\ A_1 - A_2 & A_2 \end{bmatrix} \begin{bmatrix} \delta x_1 \\ \Delta \delta x \end{bmatrix} + \begin{bmatrix} \omega_1 \\ \omega_1 - \omega_2 \end{bmatrix} \tag{18}$$

$$\begin{bmatrix} \tilde{\rho}_1 \\ \Delta \tilde{\rho} \end{bmatrix} = \begin{bmatrix} H_1 & 0 \\ H_1 - H_2 & H_2 \end{bmatrix} \begin{bmatrix} \delta x_1 \\ \Delta \delta x \end{bmatrix} + \begin{bmatrix} v_1 + b_c \\ v_1 - v_2 \end{bmatrix}. \tag{19}$$

The measurement $\Delta\tilde{\rho}$ is referred to as the single differenced GPS measurements. This term includes both the code range and Doppler measurements. The common mode errors have been eliminated in the relative measurement. In doing so, correlations between the states have been introduced. These correlations require centralized processing with a filter state twice the size of the single vehicle filter. Assuming that the two vehicles are operating along a similar trajectory, the coupling terms may be neglected. If the vehicles are close to each other (< 1 km) and traveling along a similar path, then, to first order, the dynamics of the two vehicles are equivalent. The coupling term $A_1 - A_2$ may be assumed to be zero in these circumstances. The measurement coupling $H_1 - H_2$ may also be assumed zero simply due to the proximity of the two aircraft. If correlations in the process and measurement noises are neglected, the system described in (18) and (19) may be completely decoupled into two filters.

In this case, the case of two vehicles operating along a similar trajectory, the global filter may now be separated into two separate EKF units, as described in the decentralized approach. The base vehicle and the rover operates an EKF using $\delta \dot{x}_1 = A_1 \delta x_1 + \omega_1$ as the dynamics and $\tilde{\rho}_1 = H_1 \delta x_1 + v_1 + b_c$ as the measurements. The rover vehicle now operates an EKF using $\Delta \delta \dot{x} = A_2 \Delta \delta x + \omega_1 - \omega_2$ as the dynamics and $\Delta\tilde{\rho} = H_2 \Delta \delta x + v_1 - v_2$ as the measurements.

The use of this suboptimal solution is justified as a trade between computation time, communication bandwidth, and estimation accuracy. The globally optimal filter would require 34 states and GPS as well as IMU measurements from both aircraft. This would substantially increase the computational burden and communication bandwidth requirements. The correlation between the process noise and the measurement noise is small in comparison to the benefit of eliminating the common mode errors from the relative state. Based upon these arguments, the suboptimal solution was chosen for implementation.

D. Effect of Noncollocated GPS/INS

The algorithm described applies to the case in which the GPS antenna and IMU are colocated. As discussed in Section III, the GPS and IMU are located in different parts of the aircraft. In this case, the measurement models must be modified to account for the moment arm generated by the distance between the two sensors.

The effect of the noncollocation of the GPS and INS was handled by transforming the error state, propagated at the INS location, to the GPS location using a transformation matrix. The error is then updated using the measurements in the EKF. The updated error is then transformed back to the INS location using an inverse transformation matrix [20].

E. Double Difference Carrier

The final piece in the relative navigation filter is the use of double differenced carrier phase measurements to provide precise relative positioning. These measurements are processed on the rover vehicle in addition to single differenced range and doppler. The measurements may only be processed if the integer ambiguity algorithm has converged. That algorithm is discussed in Section V. Once converged, the carrier phase measurements provide a high accuracy measurement of relative range.

There are several differences between these carrier phase measurements and the normal code range measurements. First, the double differenced measurements have a slightly different H matrix, which is composed of the difference between two of the single differenced code H matrices. To form the matrix, one satellite is declared to be the primary satellite. All of the remaining measurements are differenced with this satellite to form the double differenced measurements [17]. Second, the

double difference eliminates the effects of receiver clock bias error. However, the double difference introduces correlations into the measurement noise.

The carrier phase measurement model is defined as in (20), where one measurement comes from the prime satellite and the other from satellite i

$$\lambda(\nabla\Delta\tilde{\phi}+\nabla\Delta N)=\Delta\bar{\rho}_{\text{prime}}-\Delta\bar{\rho}_i+(H_{\text{prime}}-H_i)\Delta\delta x +\Delta v_{\text{car}_{\text{prime}}}-\Delta v_{\text{car}_i}. \quad (20)$$

The term $\nabla\Delta\tilde{\phi}$ is the double differenced carrier phase measurement, $\nabla\Delta N$ is the estimated integer ambiguity calculated in the Wald test, and λ is the wavelength of the carrier.

In order to process these measurements sequentially, the EKF uses a method in Maybeck [19] to first decorrelate the measurements and then process sequentially using the Potter scalar update.

V. Wald Test for Integer Ambiguity Resolution

This section briefly describes the method used in the FFIS to resolve the integer ambiguity so that carrier phase measurements may be used in the EKF described in the previous section. This method has been presented previously in [21] and will only be summarized here. The algorithm uses only GPS measurements and is completely independent from the GPS/INS EKF derived in the previous section. The major achievement of this algorithm is the ability to converge consistently on the correct integer ambiguity between two moving vehicles without any ground-based instrumentation.

The algorithm used is based upon the multiple hypothesis Wald sequential probability ratio test (MHWSPRT) [22]. This algorithm calculates the probability that a given integer hypothesis is true out of a set of assumed integer hypotheses in minimum time from a single residual process. The algorithm is recursive for implementation in real-time. The residual process used combines both carrier and code measurements:

$$r=\begin{bmatrix}\lambda(\nabla\Delta\tilde{\phi}+\nabla\Delta N)-\nabla\Delta\tilde{\rho}\\ E\lambda(\nabla\Delta\tilde{\phi}+\nabla\Delta N)\end{bmatrix}=\begin{bmatrix}\nabla\Delta v_{\text{car}}-\nabla\Delta v_{\text{code}}\\ E\nabla\Delta v_{\text{car}}\end{bmatrix} \quad (21)$$

where $\tilde{\phi}$ and $\tilde{\rho}$ are the carrier and code measurements, $\nabla\Delta N$ is the hypothesized integer ambiguity, and E is the left annihilator of the measurement matrix H, as in [21] and [23]. The use of the annihilator eliminates the effect of the uncertainty in the relative vehicle state on the residual process. Regardless of the initial estimate of relative range, the residual process is defined by the noise process and the integer ambiguity bias. The use of the annihilator works for relatively short baselines (<1 km).

The residual process r is a zero mean, Brownian motion process with variance given in (22)

$$\begin{bmatrix}4(V_{\text{carrier}}+V_{\text{code}}) & 16V_{\text{carrier}}E^T\\ 16EV_{\text{carrier}} & 4EV_{\text{carrier}}E^T\end{bmatrix}. \quad (22)$$

A separate residual process is generated for each hypothesized integer. Knowing the statistics, the probability density function $f_i(k+1)$ for hypothesis i at time $k+1$ may be calculated. Using this density, the probability that hypothesis i, $F_i(k+1)$, is true

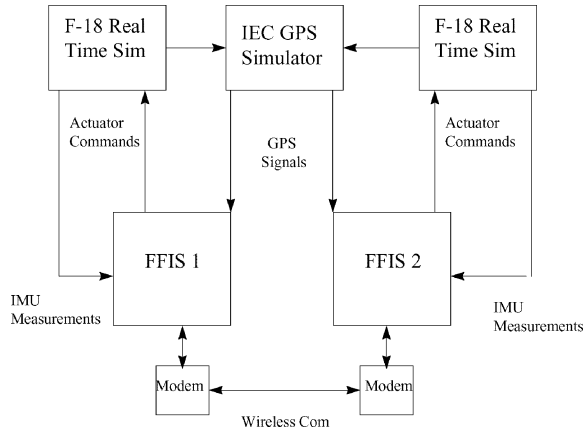

Fig. 2. FFIS HIL Sim block diagram.

is generated recursively using the following relationship. Refer to [22] and [21] for development of the algorithm

$$F_i(k+1)=\frac{F_i(k)f_i(k+1)}{\sum_{i=0}^{L}F_i(k)f_i(k+1)}. \quad (23)$$

Note that the sum of all probabilities must equal 1.0 since the algorithm assumes only one hypothesis can be true. Once a particular hypothesis reaches this value (or a threshold value), the filter declares convergence and the hypothesis meeting the value is the correct integer ambiguity.

After the Wald test converges, the integer ambiguity is maintained in a separate algorithm. Only when lock on the integer ambiguity is lost does the algorithm reset and begin to operate again. Maintenance routines determine integer biases for the remaining satellites in view using a Kalman filter that employs the high accuracy relative position resulting from the carrier phase signal [20]. This computationally low-cost method converges quickly to the correct integers without having to restart the method presented here.

The satellite with the highest elevation angle is used as the primary satellite. During the maintenance portion of the algorithm, the satellite with the second highest elevation angle is used to determine a backup, secondary integer ambiguity set in case the primary satellite is lost [20].

VI. Test Facilities

As part of the development of the FFIS, the HIL Sim facility at UCLA was developed. This facility allows the real-time test and simulation of actual flight hardware in the laboratory environment. A block diagram is presented in Fig. 2.

The simulator primarily consists of an IEC GPS constellation simulator, which outputs R/F signals to GPS receivers, simulating actual GPS signals. The IEC can simulate two vehicles with up to six channels of L1 and L2 signals for each vehicle in real-time.

The IEC is controlled by two workstations each running a nonlinear aircraft model simulation. The trajectories are run in real-time and state estimates are output from the work stations to the IEC simulator. In addition, each work station outputs analog signals directly to the FFIS in order to simulate actual IMU measurements. In this way, the FFIS units receive all of the sensor

inputs from actual flight and the algorithms and software may be tested with precision. The complete HIL Sim provides a truth model for comparison with the FFIS results. Some of these results are presented in Section VII.

VII. Flight Test Results

Flight tests of the FFIS took place at NASA Dryden Flight Research Center using NASA F-18 aircraft numbers 845 and 847. The FFIS units flew in a series of experiments starting in June of 2001 and ending in December of the same year. Results from these flight tests are summarized in this section.

A. FFIS Wald Test Results

To evaluate the Wald test performance, a least squares relative state estimate was computed using the Wald test resolved integer ambiguity and carrier phase measurements.

The Wald test was operated in real-time in the HIL Sim. In the HIL Sim, the Wald test always converged correctly. The true integer value could be calculated and verified since the true trajectory was known.

In flight, however, the evaluation process is more difficult. To evaluate the Wald test, an independent set of GPS receivers was employed to calculate the relative range between aircraft. This relative range was then compared with the least squares estimate generated from the Wald test hypotheses.

The independent system used a commercially available post-processing software package called PNAV, which is a product of Ashtech. PNAV calculates the relative position between a ground-fixed GPS receiver and a moving GPS receiver through a batch processing method. In this way, PNAV calculated the position of each aircraft relative to a fixed point on the ground at Edward's Air Force Base. The estimates of each aircraft state were differenced to generate the relative position which was compared with the Wald test least squares solution.

Since PNAV requires a base station to resolve the integer ambiguity, it uses three ASHTECH receivers, one on board each vehicle and the third is the base station receiver. The GPS receivers are not shared between the FFIS and PNAV. Thus, a total of five GPS receivers are used in the evaluation process. The error between the FFIS and PNAV is due to error in the FFIS estimate and error in the PNAV estimate. The error is expected to be larger than what most GPS manufacturers quote for differential carrier phase GPS applications because of the large number of receivers and the different levels of processing involved in this evaluation.

Fig. 3 shows the relative position error between the FFIS Wald estimate and the offline PNAV estimate. It can be seen that the FFIS real-time estimate is almost equal in mean to the PNAV estimate. This can be seen from the almost zero mean relative position error. Table II gives the mean and standard deviation for each axis in the plot. This type of error is typical for the flight tests.

In this case, the Wald test converged and the maintenance algorithms operated on the carrier phase integers so that the FFIS maintained integer lock for over 1000 s. Typically, the carrier phase integers would remain valid for 782.1 s after convergence. Convergence is only lost if the GPS receivers lose lock and only three or fewer satellites are still measured. This can

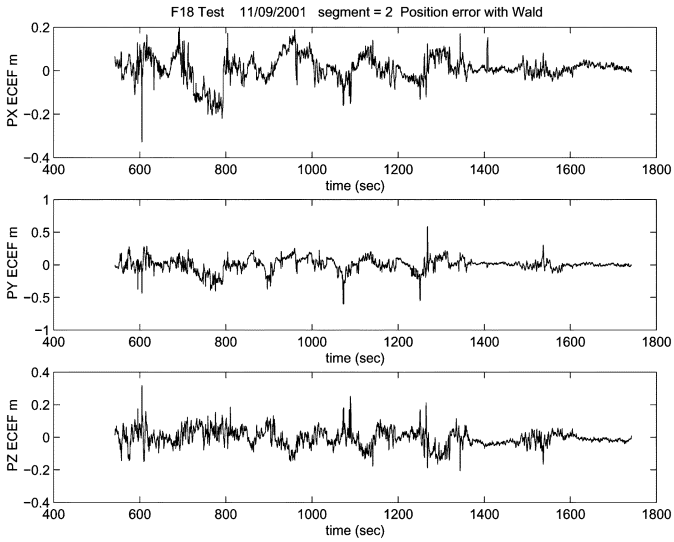

Fig. 3. Relative position estimate error from the Wald test—F18 test.

TABLE II
Representative Wald Test Error From an F-18 Test

Mean - x (m)	-0.0138	Standard Deviation - x (m)	0.0453
Mean - y (m)	-0.0497	Standard Deviation - y (m)	0.0944
Mean - z (m)	-0.0563	Standard Deviation - z (m)	0.0824

happen when high roll maneuvers are used during turns which cause satellites on the horizon to become obscured. In addition, during the last set of tests, the carrier phase integer ambiguity was locked for 87.6% of the portion of the flight in which the FFIS operated.

These results show that the Wald test did converge correctly on the F-18 aircraft and that the solution was valid for long periods of time in this highly dynamic environment. Unfortunately, the Wald test could not be proven to converge correctly during all flight tests. During some tests, the PNAV software did not converge for most of the flight making evaluation to this degree of accuracy impossible. However, when PNAV did converge, the Wald test least squares solution was at or near this level of accuracy in every case, indicating that the two methods were in agreement.

B. FFIS EKF Test Results

This section highlights some of the EKF estimate flight test results. The FFIS EKF outputs were evaluated in comparison with the same PNAV data used to evaluate the Wald test. In addition, the FFIS attitude estimates are compared with the onboard aircraft navigation system.

During flight tests, a problem was discovered with the flight qualified FFIS units. The noise level in the IMU was much larger than expected. The flight units were removed from the airplane and tested in the HIL Sim at UCLA. During these tests, it was discovered that the FFIS unit itself was generating the noise in the IMU channels. This noise level caused the estimates of the EKF to have larger error than anticipated in flight although it did operate in real-time.

For the purposes of development, UCLA owned and operated two other FFIS units that were not flight qualified. These units

TABLE III
BASE VEHICLE ERRORS FOR THE DEVELOPMENT FFIS IN THE HIL SIM

State	Mean	Std. Dev.
Pecefx(m)	4.5536	0.1734
Pecefy(m)	-28.8250	0.1765
Pecefz(m)	22.4826	0.1447
Vecefx(m/s)	-0.0131	0.0297
Vecefy(m/s)	0.0187	0.0264
Vecefz(m/s)	-0.0081	0.0283
Roll(deg)	-0.0548	0.0183
Pitch(deg)	-0.0374	0.0174
Yaw(deg)	-0.2867	0.0764
bias gyrox(deg/s)	-0.0003	0.0278
bias gyroy(deg/s)	-0.0007	0.0210
bias gyroz(deg/s)	0.0005	0.0218
bias accelx(m/s^2)	0.0011	0.0037
bias accely(m/s^2)	0.0039	0.0056
bias accelz(m/s^2)	0.0223	0.0293
raw gyrox(deg/s)	0.0022	0.0278
raw gyroy(deg/s)	-0.0000	0.0209
raw gyroz(deg/s)	-0.0006	0.0219
raw accelx(m/s^2)	-0.0020	0.0036
raw accely(m/s^2)	-0.0039	0.0055
raw accelz(m/s^2)	-0.0331	0.0293

were used in the HIL Sim and shown to meet the desired accuracies in relative navigation as opposed to the flight qualified units. The two systems were meant to be functionally equivalent in every way, but were not.

In this section, we present results that show how nonflight qualified FFIS units operated in the HIL Sim. The performance is compared with the flight qualified units in the same HIL Sim test to show the level of noise in the flight units and its effect on estimation. Finally, the best case error in the filter is presented for the flight tests. The argument is made that if the noise level is reduced in the flight qualified units, then the FFIS will operate with the expected accuracy. This claim is made based upon performance in the HIL Sim and the reasonable performance of the FFIS in actual flight tests.

1) UCLA Development FFIS HIL Sim Results: Tables III and IV give a summary of the error in the base vehicle and relative state estimates against the true trajectories. During this HIL Sim test, the aircraft both followed a similar trajectory consisting of multiple coordinated turns followed by periods of straight and level flight. Ionosphere and troposhperic errors were present in the GPS signals. The IMU model included noise levels equal to those specified by Systron-Donner (see Table I), although the true bias in each IMU measurement was zero.

The base vehicle results show very good estimation of the true state. Large biases are found in position estimates because the FFIS does not model ionosphere error. These large position errors are not considered problematic since the relative error estimation process removes the effect of the ionosphere. The velocity estimates are accurate to a few centimeters per second. The attitude estimates are accurate to less than a few tenths of a degree. Yaw is the most inaccurate because Yaw is the least observable during long periods of steady-state flight [16], [24]. All of the bias estimates show near zero mean as do the raw measurements. The raw_gyro and raw_accel states represent the error between the HIL Sim generated gyro and acceleration measurements and the actual measurements sampled in the FFIS. The noise level is slightly larger than the noise for the IMU listed in Table I.

TABLE IV
RELATIVE VEHICLE FILTER ERRORS FOR THE DEVELOPMENT FFIS IN THE HIL SIM

State	Mean	Std. Dev.
Rel. Pecefx(m)	0.0648	0.0405
Rel. Pecefy(m)	-0.1359	0.0384
Rel. Pecefz(m)	-0.0189	0.0362
Rel. Vecefx(m/s)	0.0044	0.0457
Rel. Vecefy(m/s)	-0.0078	0.0392
Rel. Vecefz(m/s)	0.0069	0.0428
Rel. Roll(deg)	-0.0009	0.0201
Rel. Pitch(deg)	0.0266	0.0227
Rel. Yaw(deg)	-0.1117	0.0777
Rel. biasgyrox(deg/s)	0.0005	0.0308
Rel. biasgyroy(deg/s)	0.0002	0.0279
Rel. biasgyroz(deg/s)	-0.0007	0.0278
Rel. biasacclx(m/s^2)	0.0055	0.0038
Rel. biasaccly(m/s^2)	0.0047	0.0045
Rel. biasacclz(m/s^2)	0.0003	0.0141

TABLE V
FLIGHT QUALIFIED FFIS BASE VEHICLES IMU ERRORS IN THE HIL SIM

State	Mean	Std. Dev.
raw gyrox(deg/s)	0.2048	1.4689
raw gyroy(deg/s)	0.1899	1.4084
raw gyroz(deg/s)	0.1564	1.4242
raw accelx(m/s^2)	0.0787	0.8324
raw accely(m/s^2)	0.0701	0.8994
raw accelz(m/s^2)	0.0959	0.8988

The relative filter estimates are computed by subtracting the output of the rover from the base. These estimates show that the relative EKF position estimates have approximately 15 cm of bias and 7 cm of standard deviation error. The relative velocity and attitude estimates are smaller than the absolute error in the base vehicle. The small error in the relative IMU bias estimates indicates that the decentralized EKF filter did estimate the bias error in the rover vehicle accurately.

2) Flight Qualified FFIS HIL Sim Results: The flight qualified FFIS units were evaluated at UCLA in the HIL Sim environment. Large bias and noise values were measured from the raw analog IMU signals. These signals aversely affected the state estimation process.

Table V summarizes the IMU performance of the base vehicle FFIS. Immediately, it may be seen that the raw_gyro and raw_accel measurements are orders of magnitude larger in both mean and variance than the development units and larger than the noise level of the IMU. This noise level indicates that the FFIS unit has an internal problem with the connection to the IMU since the same IMU noise settings were used in this test as in the test with the development FFIS units.

From this test, it was shown that the effect of large error in the IMU propagate into the other states. All of the bias estimates remain small in mean, but have large standard deviations. The same holds true for position and velocity. Attitude estimates have large errors in mean and much larger standard deviations than the development unit.

The rover FFIS unit has a similar performance and problem as the base FFIS. The results are not repeated for brevity. Table VI shows the effect of the larger IMU noise on the relative estimates. Bias estimates have a larger mean and standard deviation than the base. The relative attitude estimates have enormous bias

TABLE VI
FLIGHT QUALIFIED FFIS RELATIVE VEHICLE FILTER ERRORS IN THE HIL SIM

State	Mean	Std. Dev.
Rel. Pecefx(m)	-0.3225	0.4349
Rel. Pecefy(m)	0.9346	0.3430
Rel. Pecefz(m)	0.0422	0.6282
Rel. Vecefx(m/s)	0.1385	0.1958
Rel. Vecefy(m/s)	-0.0546	0.1794
Rel. Vecefz(m/s)	-0.0707	0.1858
Rel. Roll(deg)	-1.5339	1.1061
Rel. Pitch(deg)	-5.7012	0.8416
Rel. Yaw(deg)	-11.6662	2.7076
Rel. bias gyrox(deg/s)	-0.0508	1.6808
Rel. bias gyroy(deg/s)	0.1264	1.6870
Rel. bias gyroz(deg/s)	-0.1117	1.6762
Rel. bias acclx(m/s^2)	-1.0298	1.0571
Rel. bias accly(m/s^2)	0.5080	1.1138
Rel. bias acclz(m/s^2)	-0.1872	1.0940

TABLE VII
SUMMARY OF EKF PERFORMANCE FROM AN F-18 TEST

Variable	Mean	Std. Dev.
Rel. Range_ecefx(m)	-0.0428	0.1971
Rel. Range_ecef(m)	0.1759	0.4506
Rel. Range_ecefz(m)	0.2618	0.1888
Rel. V_east(mps)	-0.0050	0.1389
Rel. V_north(mps)	-0.0723	0.1624
Rel. V_down(mps)	-0.0514	0.1844
Rel. Pitch (deg)	-2.4582	0.8581
Rel. Roll (deg)	1.8451	1.3245
Rel. Yaw (deg)	-2.1944	0.4710

in yaw, which is the least observable state. The relative velocity and position estimates have large biases and standard deviations compared with the development units.

Based upon these results, the conclusion must be that the FFIS units have a large amount of noise compared with development units in the A/D card. This noise degrades the performance of the FFIS during HIL Sim tests. As would be expected, the performance also degrades during flight tests.

3) Flight Qualified FFIS Flight Test Results: In flight both FFIS units were able to operate, take data, and compute estimates. These estimates are compared with the PNAV data used in Section VII-A and the independent F-18 INS solution. While PNAV accuracy is similar to carrier phase GPS levels when PNAV converges, the navigation system on each aircraft was only accurate to 0.5° in each axis which was less than the anticipated FFIS accuracy. However, the high noise in the FFIS IMU measurements causes the FFIS to estimate attitude more poorly than was expected.

For the purpose of brevity, only a representative set of data is presented. This particular flight was flown on November 9, 2001. Table VII shows a summary of the relative error during a 700 s stretch of data. From this chart, the relative range bias and standard deviation are much larger than in the HIL Sim, even though carrier phase data is processed in the EKF. Fig. 4 shows a plot of the relative range during this time period. The estimates slowly drift with slight biases and large variations over the interval. This type of behavior and error level was typical during the last set of flight tests.

During smaller segments of time, the actual required accuracy was achieved briefly. During 100 s of the above segment, the

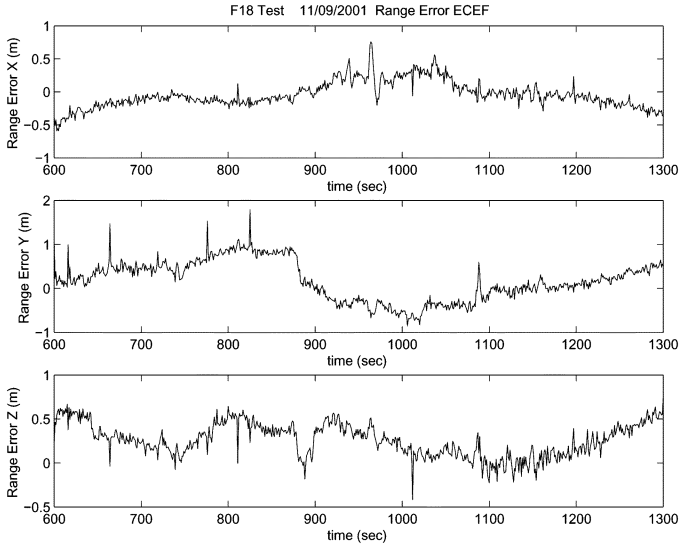

Fig. 4. Relative range estimate from the EKF—F-18 test.

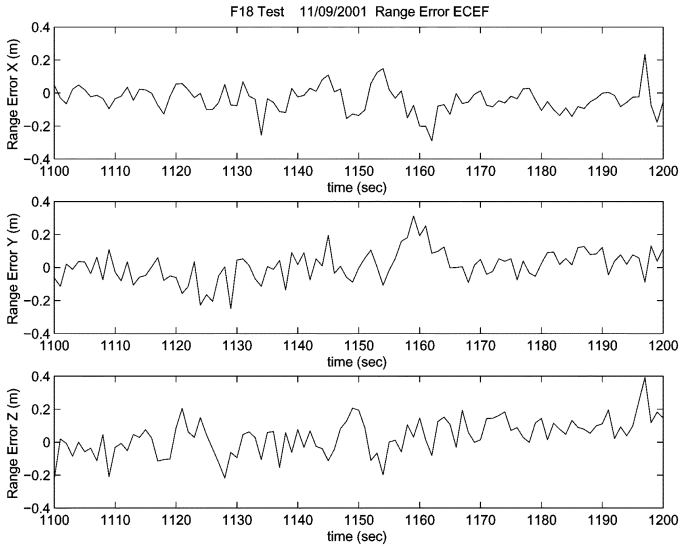

Fig. 5. Relative position estimate from the EKF (close up)—F-18 test.

mean and standard deviation of the error became as good as the HIL Sim results. This error is plotted in Fig. 5. While the FFIS was capable of meeting the requirements, the low-error level was not sustainable for long periods of time due to noise in the IMU.

Table VII also shows the mean and variance of the velocity and attitude estimates. The velocity estimates are near zero mean, but have much larger variation in error than the FFIS operating in the HIL Sim. The attitude estimates show larger error bias and standard deviations on the order of 1°–2°. Typical error in both attitude and velocity remained in this magnitude of error. As before, brief periods of exceptional performance were recorded, but not sustained.

The results presented here point to several conclusions. First, the FFIS did operate and take data in the flight environment. This is shown by these results and from the actual flight results of the Wald test presented earlier. Second, the FFIS did not sustain relative range estimates to the accuracy required using the EKF,

although it did meet the requirements using the Wald test. The third point is to note that given the results in the HIL Sim and the fact that the IMU noise was corrupted in the flight qualified FFIS units, minor adjustments to the flight qualified FFIS units should yield improved results.

Once the problem was discovered, it was not repaired in flight due to compromises in budget, schedule, and program objectives. The cost of repair in terms of schedule slip was not acceptable. However, the major program milestones, sustained relative range estimates accurate to 30 cm were already achieved using the Wald test. Therefore, no major repair was deemed necessary until the flight tests were completed.

VIII. Conclusion

A new instrument for navigation and relative navigation is presented. The system relies on a GPS/INS on each aircraft to provide measurements. A new EKF is designed to estimate the location of each aircraft relative to the other. A new integer ambiguity algorithm for estimating the GPS integer ambiguity problem was developed. The system was tested in actual F-18 aircraft.

The relative navigation system was able to estimate relative position estimates using a least squares algorithm and GPS only measurements. This system had a bias of 7 cm and a standard deviation of 13 cm as compared with a completely independent, ground-based GPS system. Further, the Wald test operated well even when the post-processing algorithm did not operate.

The FFIS EKF worked well, but did not meet accuracy goals. However, the HIL Sim tests shows that if the IMU noise level is greatly reduced, the FFIS operation should reach expected levels. The algorithms are sound and the software operates correctly. Even with a large amount of noise in the IMU, the EKF during some regions only had a mean error of 2° and a standard deviation of 1°.

The FFIS represents a significant advance in the development of relative navigation systems. The FFIS may be applied to other fields of research such as automated aerial refueling or ground-based applications such as precision farming.

Finally, the FFIS can be used to navigate multiple UAVs by grouping each two neighboring aircraft together and, therefore, a bank of relative and absolute state estimates of the aircraft is obtained and updated in real-time. In this configuration, only the leader aircraft would be operating as a base vehicle, while the rest would be operating as a follower vehicles and, therefore, will be operating a relative state estimation filter.

References

[1] I. D. Hummel, "The use of aircraft wakes to achieve power reductions in formation flight," presented at the Advisory Group for Aerospace Reasearch and Development (AGARD) Conf. Trondheim, Norway, Nov. 1996, 584.

[2] D. F. Chichka and J. L. Speyer, "Solar-powered, formation-enhanced aerial vehicle systems for sustained endurance," in *Proc. Amer. Contr. Conf.*, 1998, pp. 684–8.

[3] R. J. Ray, B. R. Cobleigh, M. J. Vachon, and C. J. St, Flight test techniques used to evaluate performance benefits during formation flight, NASA Dryden Flight Research Center, NASA/TP-2002–210730, 2002.

[4] R. N. Banavar, D. F. Chichka, and J. L. Speyer, "Convergence and synthesis issues in peak-seeking control," in *Proc. IEEE Amer. Contr. Conf.*, 28–30, 2000, pp. 438–443.

[5] D. F. Chichka, J. L. Speyer, and C. G. Park, "Peak-seeking control with application to formation flight," in *Proc. 38th IEEE Conf. Dec. Contr.*, 1999, pp. 2463–2470.

[6] J. A. Farrell, T. Givargis, and M. Barth, "Differential carrier phase gps aided ins for automotive applications," in *Proc. Amer. Contr. Conf.*, 1999, pp. 3660–3664.

[7] E. A. Olsen, C. Park, and J. P. How, "3D formation flight using differential carrier-phase GPS sensors," in *Proc. Inst. Navigation*, 1998, pp. 1947–1956.

[8] J. H. Waters, P. P. Sousa, W. L. Wellons, G. D. Colby, and J. Weir, "Test results ofan F/a-18 automatic carrier landing using shipboard relative gps," in *Proc. 57th Annu. Meeting Inst. Navigation*, 2001, pp. 841–851.

[9] P. Teunissen, "A new method for fast carrier phase ambiguity estimation," in *Proc. IEEE PLANS*, 1994, pp. 562–573.

[10] ——, "An optimality property of the integer least-squares estimator," *J. Geodesy*, vol. 73, pp. 587–593, 1999.

[11] J. A. Farrell and M. Barth, *The Global Positioning System and Inertial Navigation*. New York: McGraw-Hill, 1999.

[12] W. R. Williamson, "Real time, high accuracy, relative state estimation for multiple vehicle systems," Ph.D. dissertation, Mech. Eng. Dept., UCLA, Los Angeles, CA, 2000.

[13] W. R. Williamson, J. Min, and J. L. Speyer, "Comparison of state space, range space, and carrier phase differential gps/ins positioning," in *Proc. Amer. Contr. Conf.*, 2000, pp. 2932–2938.

[14] ——, "A comparison of an optimal global and a suboptimal decentralized differential gps/ins filter for relative state estimation," in *Proc. Inst. Navigation (ION) Techn. Meeting*, 2000, pp. 125–133.

[15] W. H. Press, S. A. Teukolsky, W. T. Vetterling, and B. P. Flannery, *Numerical Recipes in C*, Second ed. Cambridge, U.K.: Cambridge Univ. Press, 1994, pp. 710–714.

[16] S. Hong, M. Lee, J. Rios, and J.L Speyer, "Observability analysis of GPS aided ins," in *Proc. Inst. Navigation*, 2000, pp. 2618–2624.

[17] B. Hofmann-Wellenhof, H. Lichtenegger, and J. Collins, *GPS Theory and Practice*, 4th ed. New York: Springer-Verlag, 1997.

[18] B. W. Parkinson and J. J. Spiker, *Global Positioning System: Theory and Applications*. Washington, D.C: AIAA, Inc., 1996, vol. 1 and 2.

[19] P. S. Maybeck, *Stochastic Models, Estimation and Control, Volume 1*. Arlington, VA: Navtech Book and Software Store, 1994.

[20] M. F. Abdel-Hafez, "A high integrity gps/ins filter for precise relative navigation," Ph.D. dissertation, Mechanical Eng. Dept., UCLA, Los Angeles, CA, 2003.

[21] J. D. Wolfe, W. R. Williamson, and J. L. Speyer, "Hypothesis testing for resolving integer ambiguity in GPS," *Navigation: J. Inst. Navigation*, vol. 50, no. 1, pp. 45–56, 2003.

[22] D. Malladi and J. L. Speyer, "A generalized shiryayev sequential probability ratio test for change detection and isolation," *IEEE Trans. Autom. Contr.*, vol. 44, no. 8, pp. 1522–1534, Aug. 1999.

[23] C. Park, I. Kim, J. G. Lee, and G. I. Lee, "Efficient ambiguity resolution using constraint equations," in *Proc. IEEE Pos. Locat. Navigation Symp.—PLANS*, 1996, pp. 277–284.

[24] I. Rhee, M. F. Abdel-Hafez, and J. L. Speyer, "On the observability of strapdown ins system during maneuvers," *IEEE Trans. Aerosp. Electron. Syst.*, vol. 40, no. 2, pp. 526–536, Apr. 2004.

Walton R. Williamson received the B.S. degree in mechanical engineering from Stanford University, Palo Alto, CA, in 1995 and the M.S. degree and the Ph.D. degree in dynamic systems and controls from the University of California, Los Angeles (UCLA), in 1996 and 2000, respectively.

During his time at UCLA, his dissertation topic was the design, test, and implementation of a real-time, relative navigation system for formation flight using a tightly coupled GPS/INS system. He co-founded SySense Inc., in 2001. His research interests include real-time navigation, and relative navigation for autonomous aerial refueling, autonomous formation flight, and autonomous landing.

Mamoun F. Abdel-Hafez received the B.S. degree in mechanical engineering from Jordan University of Science and Technology, Irbid, Jordan, in 1997, the M.S. in mechanical engineering from the University of Wisconsin, Milwaukee, in 1999, and the Ph.D. degree in mechanical engineering from the University of California, Los Angeles (UCLA), in 2003.

He is currently an Assistant Professor in the Department of Aerospace Engineering at the American University of Sharjah, Sharjah, UAE. He has served as a Post Doctoral Research Associate in the Department of Mechanical Engineering from June 2003 to December 2003, where he was involved in a research project on fault-tolerant autonomous multiple aircraft landing. His research interests include stochastic estimation, control systems, and algorithms and applications of GPS/INS systems.

Ihnseok Rhee received the B.S and an M.S degrees in aeronautical engineering from the Seoul National University, Seoul, Korea, in 1982 and 1984, respectively, and the Ph.D degree in aerospace engineering from the University of Texas at Austin, Austin, in 1990.

He is currently a Professor in the School of Mechatronics at the Korea University of Technology and Education, Chunan Choongnam, Korea. He spent a research leave in the Mechanical and Aerospace Engineering Department of the University of California in Los Angeles, Los Angeles, during 2000–2001 and 2004–2005. His current research interests include guidance and control of aerospace and robot system and applications of GPS/INS system.

Eun-Jung Song received the B.S., M.S., and Ph.D. degrees, all in aerospace engineering, from the Korea Advanced Institute of Science and Technology, Taejon, Korea, in 1995, 1997, and 2000, respectively.

She visited the University of California at Los Angeles, Los Angeles, as a Postdoctoral Researcher from 2000 to 2001. She is currently a Senior Researcher at the Korea Aerospace Research Institute, Daejeon, Korea. Her research interests include neural networks, missile guidance, and aircraft navigation.

Jonathan D. Wolfe (M'03) received the B.S., M.S., and Ph.D. degrees, all in mechanical engineering, from the University of California, Los Angeles, in 1994, 1996, and 2001, respectively.

He is currently both a Research Engineer in the Mechanical and Aerospace Engineering Department at the University of California, Los Angeles, and a Research Engineer at SySense, Inc., Burbank, CA. His current research interests include differential GPS estimation and validation, fault-tolerant control, large scale sensor networks, and multi-player games with information constraints.

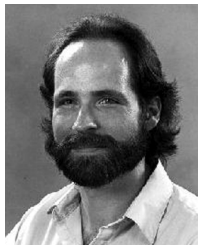

David F. Chichka (M'93) received the B.S. degree in aerospace and ocean engineering, the M.S. degree in aerospace engineering, and the B.A. degree in english from Virginia Polytechnic Institute and State University,Blacksburg, VA, in 1984, 1985, and 1986, respectively, and the Ph.D. degree in aerospace engineering from the University of California, Los Angeles (UCLA), in 1994.

From 1994 to 2002, he was a Lecturer and Research Engineer in the Mechanical and Aerospace Engineering Department at UCLA. He was also a Senior Engineer in the Control and Dynamical Systems Department at the California Institute of Technology, Pasadena, CA, from 1996 to 2001. He is currently an Assistant Professor in the Mechanical and Aerospace Engineering Department at the George Washington University, Washington, DC. His research interests include robust and adaptive control, coordinated control of multiple vehicles, orbital mechanics and satellite clusters, and bio-mimetic engineering.

Dr. Chichka has been a Visiting Professor at the University of Florida and an ASEE Summer Faculty Fellow. He is a Senior Member of the American Institute of Aeronautics and Astronautics.

Jason L. Speyer (M'71–SM'82–F'85) received the B.S. degree in Aeronautics and Astronautics from the Massachusettes Institute of Technology (MIT), Cambridge, MA, in 1960, and the Ph.D. degree in applied mathematics from Harvard University, Cambridge, MA, in 1968.

He is a Professor in the Mechanical and Aerospace Engineering Department at the University of California, Los Angeles. He has twice been an elected member of the Board of Governors of the IEEE Control Systems Society. He served as an Associate Editor for Technical Notes and Correspondence (1975–1976), Stochastic Control (1978–1979), IEEE TRANSACTIONS ON AUTOMATIC CONTROL, for the *AIAA Journal of Spacecraft and Rockets* (1976–1977), for the *AIAA Journal of Guidance and Control* (1977–1978), and for the *Journal of Optimization Theory and Applications* (1981-present).

Dr. Speyer is a Fellow of the AIAA. He is a recipient of the AIAA Mechanics and Control of Flight Award, AIAA Dryden Lectureship in Research Award, Air Force Exceptional Civilian Decoration Award (1991 and 2001), IEEE Third Millennium Medal, and membership in the National Academy of Engineering.